on photoexcitation but they rapidly form excimers. Poor quantum yields of luminescence and photocarrier generation are consequences of excimer formation. Exciplex formation enhances quantum yields of the photophysical processes. Our results also suggest that the fundamental approach to efficient photophysical processes in conjugated polymers is through control of the supramolecular structure and morphology of the materials. For example, copolymerization and side-group substitutions can be used to control interchain packing distances and the degree of intermolecular excimer formation (*35*).

REFERENCES AND NOTES

1. H. Shirakawa, E. J. Louis, A. G. MacDiarmid, C. K. Chiang, A. J. Heeger, *J. Chem. Soc. Chem. Commun.* **1977**, 578 (1977).
2. T. A. Skotheim, Ed., *Handbook of Conducting Polymers* (Dekker, New York, 1986), vols. 1 and 2.
3. J. L. Bredas and R. R. Chance, Eds., *Conjugated Polymeric Materials: Opportunities in Electronics, Optoelectronics, and Molecular Electronics* (Kluwer Academic, Dordrecht, Netherlands, 1990).
4. S. A. Jenekhe, Ed., *Macromolecular Host-Guest Complexes: Optical, Optoelectronic, and Photorefractive Properties and Applications* (Materials Research Society, Pittsburgh, PA, 1992).
5. J. S. Miller, *Adv. Mater.* **5**, 587 (1993); *ibid.*, p. 671.
6. S. R. Marder, J. E. Sohn, G. D. Stucky, Eds., *Materials for Nonlinear Optics: Chemical Perspectives* (American Chemical Society, Washington, DC, 1991).
7. A. K. Agrawal, S. A. Jenekhe, H. Vanherzeele, J. S. Meth, *J. Phys. Chem.* **96**, 2837 (1992).
8. J. H. Burroughes *et al.*, *Nature* **347**, 539 (1990).
9. G. Gustafsson *et al.*, *ibid.* **357**, 477 (1992).
10. H. Antoniadis *et al.*, *Synth. Met.* **62**, 265 (1994).
11. J. A. Osaheni, S. A. Jenekhe, J. Perlstein, *Appl. Phys. Lett.* **64**, 3112 (1994).
12. J. A. Osaheni and S. A. Jenekhe, *Macromolecules* **27**, 739 (1994).
13. N. S. Sariciftci, L. Smilowitz, A. J. Heeger, F. Wudl, *Science* **258**, 1474 (1992).
14. A. J. Heeger, S. Kivelson, R. J. Schreiffer, W. P. Su, *Rev. Mod. Phys.* **60**, 781 (1988).
15. U. Rauscher, H. Bässler, D. D. C. Bradley, M. Hennecke, *Phys. Rev. B* **42**, 9830 (1990).
16. E. L. Frankevich *et al.*, *ibid.* **46**, 9320 (1992).
17. J. W. P. Hsu, M. Yan, T. M. Jedju, L. J. Rothberg, B. R. Hsieh, *ibid.* **49**, 712 (1994).
18. Z. G. Soos, S. Etemad, D. S. Galvao, S. Ramasesha, *Chem. Phys. Lett.* **194**, 341 (1992).
19. Th. Förster and K. Kasper, *Z. Phys. Chem.* **1**, 275 (1954).
20. M. Gordon and W. R. Ware, Eds., *The Exciplex* (Academic Press, New York, 1975).
21. Th. Förster, *ibid.*, pp. 1–21.
22. M. A. Winnik, Ed., *Photophysical and Photochemical Tools in Polymer Science* (Reidel, Dordrecht, Netherlands, 1986), pp. 15–42.
23. J. B. Birks, in (*20*), pp. 39–73.
24. A. Weller, *ibid.*, pp. 23–38.
25. J. Guillet, *Polymer Photophysics and Photochemistry* (Cambridge Univ. Press, Cambridge, 1985).
26. S. L. Mattes and S. Farid, *Science* **226**, 917 (1984).
27. M. A. Fox and P. F. Britt, *Macromolecules* **23**, 4533 (1990).
28. J. A. Osaheni and S. A. Jenekhe, *Chem. Mater.* **4**, 1283 (1992).
29. M. F. Roberts, S. A. Jenekhe, A. Cameron, M. McMillan, J. Perlstein, *ibid.* **6**, 658 (1994).
30. The synthesis and characterization of the molecular and supramolecular structures of the conjugated polymers have been reported (*28, 29*). These polymers are soluble in MSA and nitromethane-$AlCl_3$ in which they form liquid crystalline phases at high solution concentrations ($>\sim$5 to 10% by weight) as a result of their rigid rodlike conformations (*29*). Polymer thin films were prepared by spin casting from $\sim$0.5 to 1.0% by weight solutions in nitromethane-$AlCl_3$ as described in (*28*). Thin films of solid solutions of a conjugated polymer in poly(benzobisthiazole decamethylene) were similarly prepared through solutions in nitromethane-$AlCl_3$. We prepared the D/A bilayer thin films by first spin-casting the conjugated polymer layer (A, 15 to 40 nm thick) and then the D layer as described in (*11*).
31. J. N. Demas and G. A. Crosby, *J. Phys. Chem.* **75**, 991 (1971).
32. G. G. Guilbault, Ed., *Practical Fluorescence* (Dekker, New York, 1990), chaps. 1 and 4.
33. I. R. Gould, D. Noukakis, J. L. Goodman, R. H. Young, S. J. Farid, *J. Am. Chem. Soc.* **115**, 3830 (1993).
34. K. Zachariasse, in (*20*), pp. 275–303.
35. S. A. Jenekhe and J. A. Osaheni, *Bull. Am. Phys. Soc.* **39**, 505 (1994); in preparation.
36. This research was supported by the NSF (grant CTS-9311741), the Center for Photoinduced Charge Transfer (grant CHE-9120001), and the Office of Naval Research. We acknowledge helpful discussions with H. Antoniadis and S. Farid.

31 March 1994; accepted 16 June 1994

The Molecular Fossil Record of Oleanane and Its Relation to Angiosperms

J. Michael Moldowan,* Jeremy Dahl,† Bradley J. Huizinga,‡
Frederick J. Fago,† Leo J. Hickey, Torren M. Peakman,
David Winship Taylor

Oleanane has been reported in Upper Cretaceous and Tertiary source rocks and their related oils and has been suggested as a marker for flowering plants. Correspondence of oleanane concentrations relative to the ubiquitous microbial marker 17α-hopane with angiosperm diversification (Neocomian to Miocene) suggests that oleanane concentrations in migrated petroleum can be used to identify the maximum age of unknown or unavailable source rock. Rare occurrences of pre-Cretaceous oleanane suggest either that a separate lineage leads to the angiosperms well before the Early Cretaceous or that other plant groups have the rarely expressed ability to synthesize oleanane precursors.

Oleananes are diagenetic alteration products of oleanane and taraxerene precursors (*1*), which in modern plants, except for a lichen (*2*) and a few related fern species (like *Polypodium* and *Marsilea*) (*3, 4*), are concentrated among the angiosperms (flowering plants) (*5*). Oleananes in rock extracts and petroleum are also thought to derive from angiosperms (*6*) and have been reported in numerous sources worldwide (*7–11*).

Undoubted angiosperm fossils are unknown earlier than the Early Cretaceous (*12, 13*). However, some fossil remains and cladistic analyses imply that angiosperms originated in the Triassic (*14, 15*), and studies with chloroplast DNA sequences and angiosperm DNA nucleotide sequences set angiosperm evolution to 200 million years ago (*16*) to more than 300 million years ago (*17, 18*), respectively. In any case, angiosperms were sparse in Early Cretaceous floras and begin dominating floras by the beginning of the Late Cretaceous (*19, 20*). Early Cretaceous angiosperm fossils have an extremely narrow range of variation (*12, 21*) and are scarce, a condition that may reflect a sparse population and herbaceous habit with relatively weak construction compared with their shrubby or arborescent descendants (*22*). Other studies yield a similar pattern (*23, 24*) with low occurrence of angiosperms during the Early Cretaceous but a major increase during the Late Cretaceous and early Tertiary.

The problematic evolutionary history of angiosperms and their probable connection with oleananes prompted us to study the occurrence of oleananes in rock extracts. Two components were necessary to implement this study: (i) a rapid quantitative analytical method providing firm oleanane determinations at low concentrations and (ii) a large, diverse sample suite of biostratigraphically well-defined, organic-rich, finegrained sedimentary rocks.

Commonly used techniques for oleanane

J. M. Moldowan, Department of Geological and Environmental Sciences, Stanford University, Stanford, CA 94305–2115, USA.
J. Dahl, B. J. Huizinga, F. J. Fago, Chevron Petroleum Technology Company, Post Office Box 1627, Richmond, CA 94802–0627, USA.
L. J. Hickey, Department of Geology and Geophysics, Post Office Box 208109, Yale University, New Haven, CT 06520–8109, USA.
T. M. Peakman, School of Chemistry, University of Bristol, Cantock's Close, Bristol, England BS8 1TS.
D. W. Taylor, Department of Biology, Indiana University, S.E., 4201 Grant Line Road, New Albany, IN 47150, USA.

---

*To whom correspondence should be addressed.

†Present address: Department of Geological and Environmental Sciences, Stanford University, Stanford, CA 94305–2115, USA.

‡Present address: ARCO International Oil and Gas Company, 2300 W. Plano Parkway, Plano, TX 75075, USA.

identification are unreliable when applied to samples containing zero to small amounts of oleanane (*25*). For rock extracts and petroleum saturate hydrocarbon fractions, oleanane is typically analyzed by gas chromatography–mass spectrometry (GC-MS) selected ion monitoring (SIM) of the *m/z* 191 and other fragments. However, other pentacyclic triterpanes with similar retention times and insufficiently distinguishable mass spectra occur in small amounts in rocks and can interfere with SIM–GC-MS analysis (*25*), prompting us to develop a more selective analysis based on metastable reaction monitoring (MRM) GC-MS (Fig. 1) (*26*).

We focused on Jurassic through Miocene age rock samples deposited in marine to marine-deltaic environments. Rocks from these environments contain organic matter derived from a variety of terrestrial sources, in contrast to nonmarine coal, swamp, fluvial, and lacustrine deposits that tend to focus terrestrial input from local environments. Samples came from cores, side-wall cores, or outcrops, with total organic carbon contents $\geq$1% by weight, and the samples were thermally mature on the basis of kerogen pyrolysis (*27*).

Absolute concentrations of oleanane poorly reflect the level of input of oleanane precursors because concentrations of biological markers can vary by several orders of magnitude, depending mostly on the thermal maturity of the sample (*28*). Therefore, we used the ratio of the sum of the 18α- and 18β-oleananes to 17α-hopane calculated from the convenient major metastable transition for both molecular types, *m/z* 412→191. The compound 17α-hopane, which is derived from stereoisomerization of hopanols present in most classes of bacteria (*29*), is found in all rock extracts and petroleum (*30*), except those that have been altered by heavy biodegradation or extreme thermal maturity (*28*). Furthermore, because of the similarity in structure and stability between oleanane and hopane, the effects of thermal maturation are minimized by use of a ratio.

The results of the oleanane analyses are broadly comparable with those found for fossil angiosperm occurrences (Fig. 2). The relative concentrations of oleanane to hopane, excluding the unusual Middle Jurassic and Neocomian occurrences (see later), begin low, near the detectable limit of 3% during the Early Cretaceous and steadily increase to a plateau during the latest Cretaceous. Then, during the Tertiary there is a major increase. The frequency values (Fig. 2) are low during the Jurassic and Early Cretaceous and increase steadily until the first part of the Late Cretaceous. The major increase occurs during the end of the Late Cretaceous, with a continued increase during the Tertiary.

There appears to be a relation between angiosperm taxonomic diversification and the concentration and frequency of oleanane occurrence. Yet there are several important differences. Whereas the major increases in taxonomic diversification of genera occur during the mid-Cretaceous (*19, 20*), major increases in oleanane frequencies occur during the latest Cretaceous, and the major increases in oleanane concentrations are even later. We suggest two possibilities that could account for this.

First, the quantitative oleanane record may represent the chemical signature of the quantitative increase in angiosperm biomass through geological time. These oleanane data also suggest that increases in angiosperm biomass and ecological dominance occurred later than taxonomic diversification. This fits well with the suggestion that angiosperms had an herbaceous origin (*22, 31*) and with the data that large pieces of angiosperm wood are rare until the Late Cretaceous (*32*), but even then, floras seem to have been composed of predominately herbaceous angiosperms (*33*). This is sup-

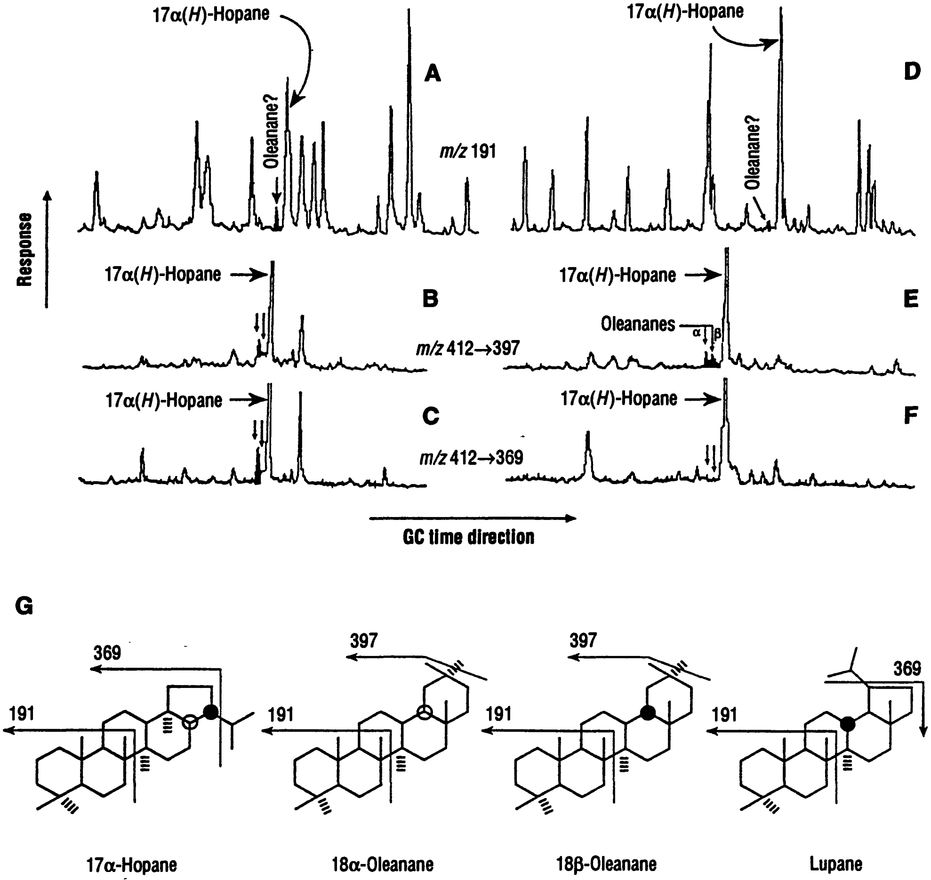

Fig. 1. Analysis for oleananes relative to hopane using selected metastable transitions (MRM) compared with SIM GC-MS. (**A**) SIM GC-MS *m/z* 191 analysis of a Santonian marine mudstone core (70 to 80 f) extract saturate fraction from the Upper Hilliard Formation, Blazon Gap 39, Lincoln County, Wyoming, U.S.A. (sample no. 583). For chromatography we used He carrier gas and a 60-m DB-1 (J & W Scientific) fused silica capillary column on a Finnigan 4000 GC-MS system. The position of a possible oleanane peak is indicated. (**B** and **C**) MRM GC-MS *m/z* 412→397 and 369 analysis of Wyoming sample no. 583. Data were acquired with similar chromatographic conditions as in (A) except that we used H_2 carrier gas on a VG Micromass model 7070H mass spectrometer GC-MS system. The single possible oleanane peak elutes between expected positions for elutions of 18α- and 18β-oleananes indicated by small arrows. The relatively large *m/z* 369 peak (C) for this compound indicates loss of a C_3H_7 side chain uncharacteristic of oleanane which is therefore considered not detected in this sample. (**D**) SIM GC-MS *m/z* 191 analysis of Campanian calcareous marine shale outcrop extract and saturates from the Lower Naparima Hill Formation, Trinidad (sample no. A384). Experimental conditions were the same as in (A). (**E** and **F**) MRM GC-MS *m/z* 412→397 and 369 analysis of Trinidad sample no. A384. Experimental conditions were the same as in (B and C). The doublet of 18α- and 18β-oleanane is best seen in *m/z* 412→397 (E) and is also observed in *m/z* 412→191 (*43*) which is used for quantitation. Absence of peaks at oleanane retention time in *m/z* 412→369 (F) confirms oleanane identification. The 17α-hopane peak is truncated at half height in each MRM chromatogram (B, C, E, and F). (**G**) Structures of compounds mentioned in the text, including some important mass spectral fragments monitored in (A) to (F). All have *m/z* 412 molecular ions.

ported by oleanane data suggesting relatively low but increasing biomass through the Cretaceous.

A second possibility is that the late oleanane increase reflects increased use of oleanane-type compounds by angiosperms, or increased diversification into subgroups that use them. Oleanane-type compounds are common and they are important defense compounds. This also suggests that angiosperm taxa containing oleanane-type compounds existed at least during the Early Cretaceous. The later major increases could be due to the greater abundance of these compounds in derived tricolpate dicotyledons and thus may reflect the similarity of the oleanane concentration curve to that of the diversification of modern families (Fig. 2) (*34*). Obviously both possibilities may coexist. Thus, the increased frequency of appearance and initial increase in concentration would be related to increases in biomass, whereas later increases would be due to diversification of oleanane-containing groups.

The oldest Cretaceous occurrence in our study is in an outcrop sample from the Paja Formation, Upper Magdalena Basin, Colombia, which is biostratigraphically constrained to late Hauterivian to late Berriasian (~Neocomian). Its oleanane ratio [oleananes/(oleananes + hopanes)] (0.13) is inordinately high compared with the angiosperm species diversity trend line (Fig. 2, feature b). This sample had the highest oleanane ratio among 10 outcrop samples analyzed from the Upper Magdalena region that range in age from late Campanian to Neocomian. A Late Oligocene side-wall core sample from the Lower Congo Basin, Angola (Fig. 2, feature c), shows the highest relative amounts of oleanane. This value could be related to an unusually high biomass of angiosperms in this region during the Late Oligocene.

A Middle Jurassic marine siltstone from West Siberia, Russia (*35, 36*), had relatively high concentrations of oleanane (Fig. 2, feature a). We also isolated 18α-oleanane from the extract of a Pennsylvanian coal ball, a calcium carbonate concretion containing well-preserved plant material from Illinois, United States. (Fig. 3). Unlike the marine sediments, the coal ball represents localized input of vascular plants from a relatively narrow selection of species. Thus, at least two samples show oleanane that predates the earliest accepted angiosperm fossil. Implications of oleanane in these samples are unclear. Possibilities include (i) a separate lineage leading to the angiosperms [such as stem-angiophytes (*14, 37*)] left its chemical signature long before plants with unmistakably angiospermous features were preserved, (ii) that related angiosperm sister groups may have produced these oleanane-

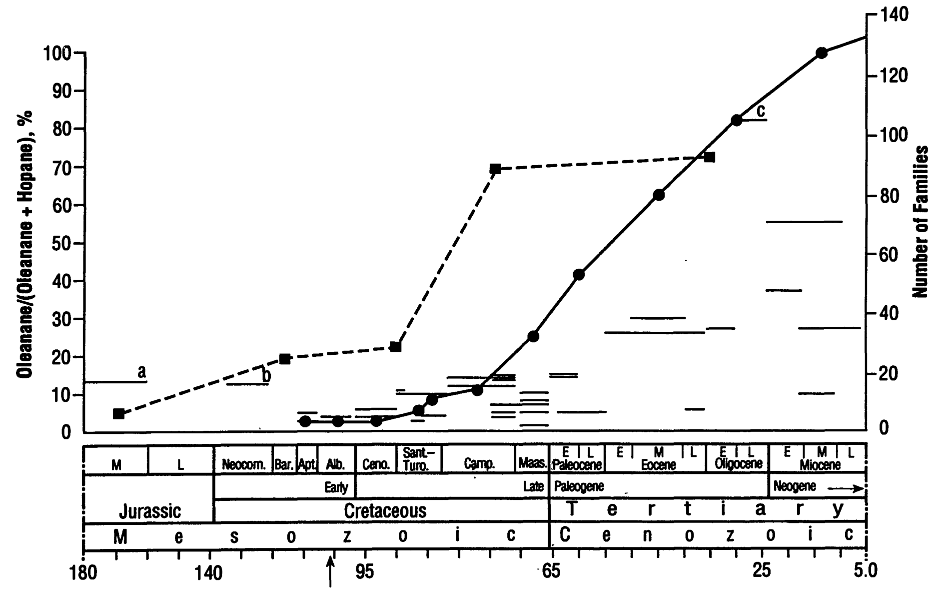

Fig. 2. Comparison with geologic time of the diversity of angiosperm families, relative amounts of oleanane, and its frequency of occurrence for 103 rock samples. Horizontal lines indicate oleanane amounts in rock samples where oleanane was detected and are expressed as percentage of 18α- + 18β-oleanane in the sum of 18α- + 18β-oleanane + 17α-hopane from MRM GC-MS, *m/z* 412→191 chromatographic peak areas. The lower detection limit is ~3% for oleanane, and samples with <3% are not indicated. The lengths of horizontal lines indicate the uncertainty of biostratigraphic determination of sample age. Specific examples discussed are (a) Middle Jurassic marine siltstone core (2409 to 2426 m), Em-Egovskaya-15, West Siberia, Russia; (b) late Hauterivian to late Berriasian [~Neocomian (Neocom.)] marine mudstone outcrop, Paja Formation, Upper Magdalena Basin, Colombia; and (c) Late Oligocene marine claystone side-wall core (8798 f), Malembo Formation, Lower Congo Basin, Angola. Squares and dashed line give frequency (%) of occurrence of detectable oleanane in portions of geological time. Each solid square represents ~20 samples for the following time spans: Jurassic, Early Cretaceous, Cenomanian (Ceno.)–Santonian (Sant.), Campanian (Camp.)–Maastrichtian (Maas.), and Paleocene-Miocene. Circles and solid line give the number of fossil pollen reports assignable to extant angiosperm families according to Muller (*24*). Note that the time scale changes at the arrow. Abbreviations: E, early; M, middle; L, late; Bar., Barremian; Apt., Aptian; Alb., Albian; Turo., Turonian.

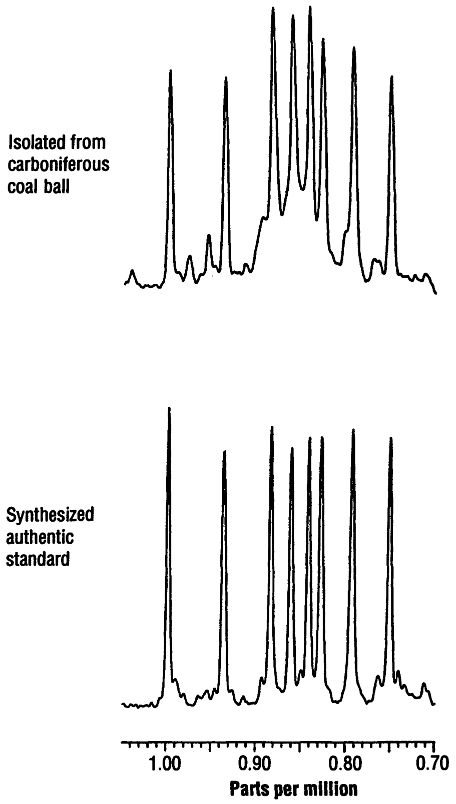

Fig. 3. Partial 400-MHz ^{1}H nuclear magnetic resonance spectra showing the methyl group resonances of authentic and isolated 18α-oleanane. Data were obtained on a Jeol GX400 spectrometer in $CDCl_3$ over the range δ 0.5 to 9.5 parts per million (ppm) with 16,384 data points, an accumulation time of 2.048 s, and a pulse delay of 1.000 s. The acquired free induction decays were zero-filled and Fourier-transformed with a Gaussian window function, and the resulting spectra referenced to residual $CHCl_3$ at δ 7.26 ppm. Authentic 18α-oleanane was run as a 0.4-mmol solution with 2400 accumulations, and isolated 18α-oleanane, as a 0.08-mmol solution with 12,000 accumulations. This confirms the identification of pre-Cretaceous 18α(*H*)-oleanane in an extract of Pennsylvanian age. The coal ball used in this analysis (Yale-Peabody Museum, YPM 8436) was found in the Sahara Coal Mine, 4 miles (6.4 km) north of Carrier Mills, Illinois, United States, and occurred in the Herrin (no. 6) coal of the Carbondale Formation, Kewanee Group, of the middle Pennsylvanian period (late Desmoinsian age–late Westphalian D) (*44*), dating to about 307 Ma (*45*).

type compounds (*38*), or (iii) that the signal is from other plants that rarely synthesize oleanane precursors.

Finally, this data set introduces the quantitative use of the oleanane parameter in assessing angiosperm input to petroleum sources. Petroleum with measurable oleanane has almost certainly been generated from Cretaceous or younger source rocks, whereas that with an oleanane ratio >0.2 was probably derived from Tertiary sources.

REFERENCES AND NOTES

1. H. L. ten Haven and J. Rullkötter, *Geochim. Cosmochim. Acta* **52**, 2543 (1988).
2. T. Bruun, *Acta Chem. Scand.* **8**, 1291 (1954).
3. H. Ageta and Y. Arai, *Phytochemistry* **22**, 1801 (1983).
4. ______, *Shoyakugaku Zasshi* **38**, 46 (Japanese, 1984).
5. M. C. Das and S. B. Mahato, *Phytochemistry* **22**, 1071 (1983).
6. E. V. Whitehead, in *Proceedings of Symposium on Hydrogeochemistry and Biogeochemistry*, Tokyo, Japan, 9 September 1970; E. Ingerson, Ed. (Clarke, Washington, DC, 1973), vol. II, pp. 158–211.
7. P. J. Grantham, J. Posthuma, A. Baak, in *Advances in Organic Geochemistry 1981*, M. Bjorøy *et al.*, Eds. (Wiley, Chichester, United Kingdom, 1983), pp. 675–683.
8. A. Riva, P. G. Caccialanza, F. Quagliaroli, *Org. Geochem.* **13**, 671 (1988).
9. M. R. Mello, P. C. Gaglianone, S. C. Brassell, J. R. Maxwell, *Mar. Petrol. Geol.* **5**, 205 (1988).
10. X. Zeng, S. Liu, S. Ma, in *Geochemical Biomarkers*, T. F. Yen and J. M. Moldowan, Eds. (Harwood Academic, Chur, Switzerland, 1988), pp. 25–49.
11. J. Fu and G. Sheng, *Appl. Geochem.* **4**, 13 (1989).
12. J. A. Doyle and L. J. Hickey, in *Origin and Early Evolution of Angiosperms*, C. B. Beck, Ed. (Columbia Univ. Press, New York, 1976), pp. 139–206.
13. N. F. Hughes, A. B. McDougall, J. L. Chapman, *J. Micropalaeontol.* **10**, 75 (1991).
14. J. A. Doyle and M. J. Donoghue, *Paleobiology* **19**, 141 (1993).
15. B. Cornet, *Mod. Geol.* **19**, 81 (1993).
16. K. H. Wolf, M. Gouy, Y. Yang, P. M. Sharp, W. Li, *Proc. Natl. Acad. Sci. U.S.A.* **86**, 6201 (1989).
17. W. Martin *et al.*, *Nature* **339**, 46 (1989).
18. W. Martin *et al.*, *Mol. Biol. Evol.* **10**, 140 (1993).
19. S. Lidgard and P. R. Crane, *Nature* **331**, 344 (1988).
20. P. R. Crane and S. Lidgard, *Science* **246**, 675 (1989).
21. L. J. Hickey and J. A. Doyle, *Bot. Rev.* **43**, 3 (1977).
22. D. W. Taylor and L. J. Hickey, *Syst. Evol.* **180**, 137 (1992).
23. K. J. Niklas, in *Patterns and Processes in the History of Life*, D. M. Raup and D. Jablonski, Eds. (Springer-Verlag, Berlin, 1986), pp. 383–405.
24. J. Muller, *Bot. Rev.* **47**, 1 (1981).
25. J. M. Moldowan, F. J. Fago, B. J. Huizinga, S. R. Jacobson, in *Organic Geochemistry. Advances and Applications in the Natural Environment*, D. A. C. Manning, Ed. (Manchester Univ. Press, Manchester, 1991), p. 195.
26. Major features of the mass spectra of 17α-hopane, lupane, 18α-oleanane, and 18β-oleanane (Fig. 1G) are remarkably similar, and various isomers or stereoisomers of hopane and lupane may coelute with the oleananes. With MRM GC-MS it was possible to take advantage of a small transition from the *m/z* 412 molecular ion (M^+) to the side-chain loss fragment *m/z* 369 that occurs in the spectra of 17α-hopane and lupane but is absent in the spectra of the oleananes. Other differences include a somewhat higher *m/z* 412→397 transition (loss of methyl) for the oleananes and the fact that oleananes typically occur as 18α and 18β isomers that can be partially resolved under the appropriate analytical conditions. The 18α to 18β isomer ratio can also be used as a maturity parameter (*8, 39*). MRM GC-MS analysis of a Wyoming shale (Fig. 1, A to C) detected an oleanane impostor, whereas analysis of a Trinidad shale (Fig. 1, D to F) detected low concentrations of oleananes.
27. Because immature shales in the Niger Delta were shown to have somewhat higher relative amounts of oleananes than mature ones (*40*), we used artificial maturation by pyrolysis to minimize the possible problems of comparing immature and mature samples. Analytical pyrolysis was carried out on crushed whole rock with commercial Rock-Eval instruments in which maximum generation (T_{max}) from the kerogen at temperatures <435°C is considered immature (*28*). Immature samples were crushed and pyrolyzed in evacuated sealed tubes at 300°C for 72 hours. Crushed rocks and pyrolyzed rocks were solvent extracted, and the extracts were fractionated by high-performance liquid chromatography (HPLC) as described (*28*). The HPLC-fractionated saturated hydrocarbons were analyzed for oleananes by MRM GC-MS (Fig. 1).
28. K. E. Peters and J. M. Moldowan, *The Biomarker Guide. Interpreting Molecular Fossils in Petroleum and Ancient Sediments* (Prentice-Hall, Englewood Cliffs, NJ, 1993).
29. M. Rohmer, P. Bisseret, S. Neunlist, in *Biological Markers in Sediments and Petroleum: A Tribute to Wolfgang K. Seifert*, J. M. Moldowan, P. Albrecht, R. P. Philip, Eds. (Prentice-Hall, Englewood Cliffs, NJ, 1992), p. 1.
30. G. Ourisson and P. Albrecht, *Acc. Chem. Res.* **25**, 398 (1992).
31. D. W. Taylor and L. J. Hickey, *Science* **247**, 702 (1990).
32. E. F. Wheeler, M. Lee, L. C. Mattern, *Bot. J. Linn. Soc.* **95**, 77 (1987).
33. S. L. Wing *et al.*, *Nature* **363**, 342 (1993).
34. Oleanane-triterpenoids and triterpenoid saponins are found throughout the angiosperms including monocot and dicot subclasses. They are most frequently found in members of the Dilleniidae, Rosidae, and Asteridae (*5, 41*). In the poorly sampled Magnoliidae (sensu Cronquist), these compounds are found throughout the herbaceous Ranunculales, although not in several woody magnolids (*42*). Further study of magnoliidean and gnetophyte phytochemistry is necessary to fully elucidate the distribution of oleanane-type compounds in living angiosperms. Finally, oleanane has been reported from the bennettitaleans, an extinct angiosperm sister group (*38*).
35. K. E. Peters *et al.*, *Am. Assoc. Pet. Geol. Bull.* **77**, 863 (1993).
36. A. E. Kontorovich *et al.*, *Sov. Geol. Geophys.* **32**, 1 (1991).
37. P. R. Crane, *Nature* **366**, 631 (1994).
38. D. W. Taylor, J. M. Moldowan, L. J. Hickey, 5th N. Amer. Paleontol. Conv. Abstr. Prog., *Paleontol. Soc. Spec. Pub.* **6**, 286 (1992).
39. C. M. Ekweozor and O. T. Udo, in *Advances in Organic Geochemistry 1987*, L. Matavelli and L. Novelli, Eds. (Pergamon, Terrytown, NY, 1988), pp. 131–140.
40. O. T. Udo and C. M. Ekweozor, *Energy Fuels* **4**, 248 (1990).
41. P. Pant and R. P. Rastogi, *Phytochemistry* **18**, 1095 (1979).
42. N. Basu and R. P. Rastogi, *ibid.* **6**, 1249 (1967).
43. J. M. Moldowan *et al.*, data not shown.
44. T. L. Phillips and W. A. DiMichele, in *Paleobotany, Paleoecology, and Evolution*, K. D. Niklas, Ed. (Praeger, New York, 1981), vol. 1, p. 231.
45. W. B. Harland *et al.*, *A Geologic Time Scale 1989*, (Cambridge Univ. Press, Cambridge, 1990).

46. We thank S. R. Jacobson for helpful discussions, C. Y. Lee and Q. Houh for sample preparations, M. M. Peña and P. Novotny for data acquisition, and Chevron Petroleum Technology Company for support of the work and permission to publish.

22 February 1994; accepted 31 May 1994

The Temporal Distribution of Seismic Radiation During Deep Earthquake Rupture

Heidi Houston and John E. Vidale

The time history of energy release during earthquakes illuminates the process of failure, which remains enigmatic for events deeper than about 100 kilometers. Stacks of teleseismic records from regional arrays for 122 intermediate (depths of 100 to 350 kilometers) and deep (depths of 350 to 700 kilometers) earthquakes show that the temporal pattern of short-period seismic radiation has a systematic variation with depth. On average, for intermediate depth events more radiation is released toward the beginning of the rupture than near the end, whereas for deep events radiation is released symmetrically over the duration of the event, with an abrupt beginning and end of rupture. These findings suggest a variation in the style of rupture related to decreasing fault heterogeneity with depth.

The fundamental processes of earthquake initiation and termination are not well understood. The details of faulting are obscured by noise in seismograms, including the incoherence of the high-frequency wave field. In addition, it is difficult to simulate earthquake faulting adequately in the laboratory because of problems of scale, temperature, and pressure. Although the failure mechanism that generates deep seismicity remains unknown (*1*), it is likely that it and the rupture process change with depth in the Earth because ambient pressure and temperature increase with depth, H_2O and CO_2 fluids are predicted to disappear below $\sim$300 km (*2*), and phase changes may play a role in rupture at great depths (*3–7*). Furthermore, the source characteristics of earthquakes with depths greater than about 100 km are more easily studied

---

H. Houston, Institute of Tectonics, Earth Sciences Department, University of California, Santa Cruz, CA 95064, USA.

J. E. Vidale, United States Geological Survey, 345 Middlefield Road, Menlo Park, CA 94025, USA.